Figure S1

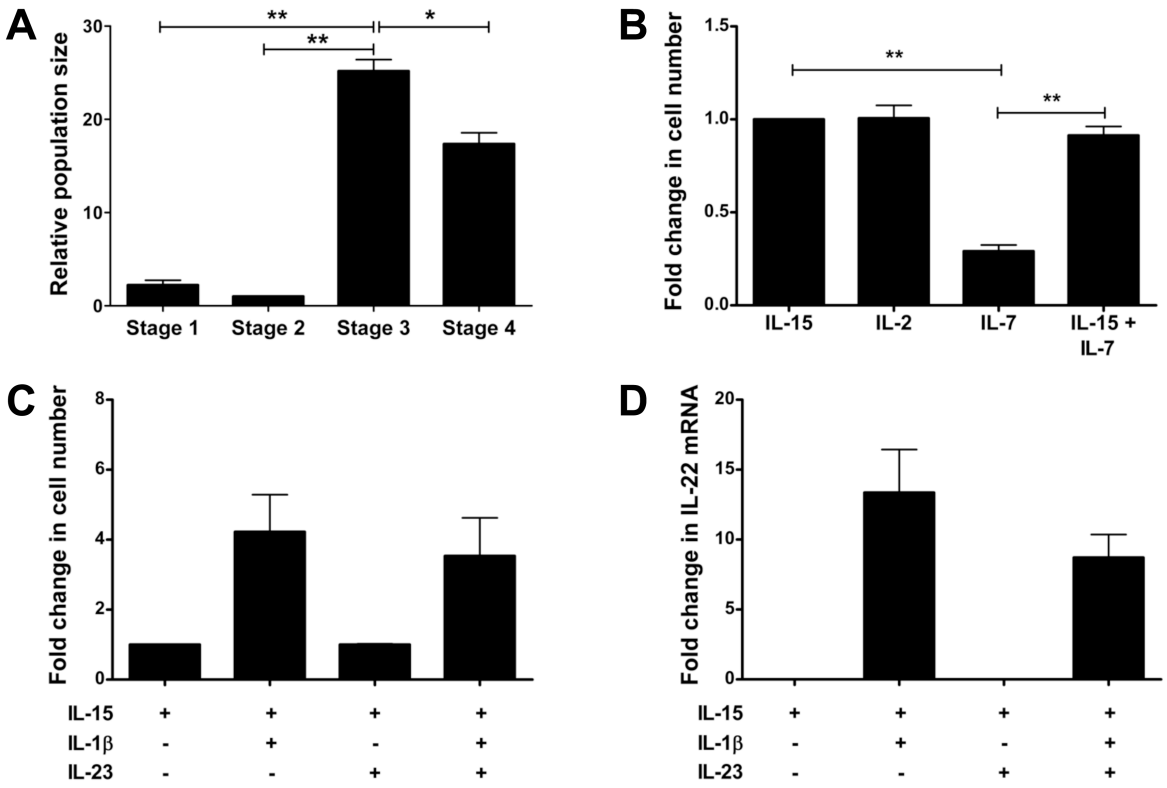

Figure S1 (related to Figure 1): Relative Abundance Ex Vivo, and Cytokine Responsiveness In Vitro, of SLT NK Developmental Intermediates

(A) Immediately after flow cytometric sorting, viable stage 1-4 NK developmental intermediates recovered from SLT of each donor were enumerated by Trypan blue exclusion. "Relative population size" was calculated within each donor as the ratio of viable cells isolated from each stage relative to the quantity in stage 2. Stage 2 cells were typically outnumbered by stages 1 (2.23 ± 0.73-fold), 3 (25.18 ± 1.74-fold) and 4 (17.35 ± 1.71-fold) (*, $P < 0.05$; **, $P \leq 0.005$).

(B-D) Total stage 3 iNK cells were purified via flow cytometry and cultured for: (B) 7 d with IL-2 (1 nM, Hoffman LaRoche), IL-7, IL-15 + IL-7, or IL-15 alone; or (C,D) 14 d with IL-15 alone, IL-15 + IL-1β, IL-15 + IL-23 (10 ng/ml R&D Systems), or IL-15 + IL-1β + IL-23. Quantity of viable cells generated *in vitro* (measured via Trypan blue assay) is depicted as "fold change in cell number", calculated as the ratio of viable cells generated from culture in each experimental condition relative to the number of cells generated from control culture with IL-15 alone.

(B) In contrast to IL-15 or IL-2, IL-7 was insufficient to maintain stage 3 iNK cell survival (**, $P \leq 0.005$).

(C and D) In the presence of IL-15 or IL-15 + IL-1β, the addition of IL-23 had no significant effect ($P \geq 0.5$) on (C) cell quantity, or (D) *IL-22* mRNA expression levels. "Fold change in *IL-22* mRNA" calculated relative to expression in parallel cultures with IL-15 alone. Results depicted as mean ± SEM ($n \geq 4$ for each).

Figure S2

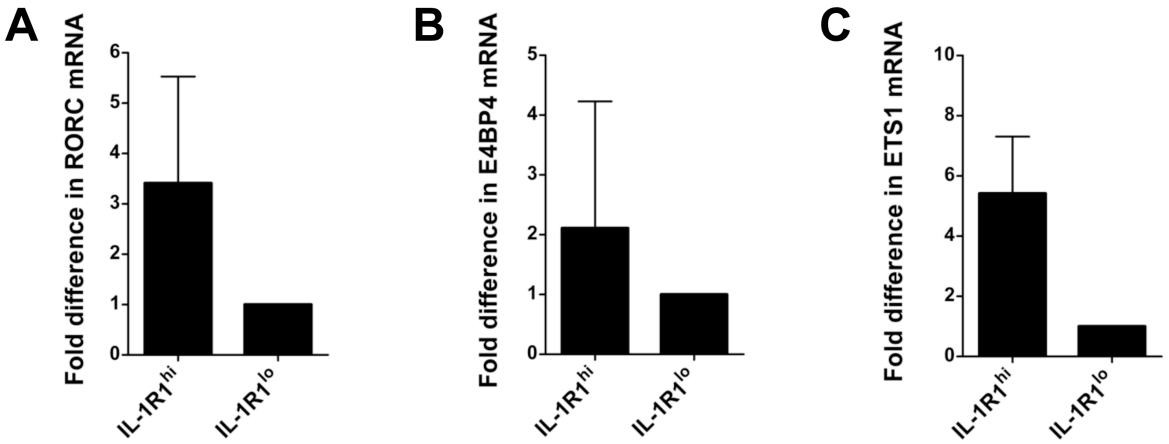

Figure S2 (related to Figure 2): Transcription Factor Expression Within IL-1R1^{hi} and IL-1R1^{lo} Subpopulations of Stage 3 iNK Cells Ex Vivo

IL-1R1^{hi} and IL-1R1^{lo} subpopulations of stage 3 iNK cells were sorted via flow cytometry for quantitative assessment of (A) *RORC* (primer and probe sequences as previously described by (Yang et al., 2006)), as well as (B) *E4BP4* and (C) *ETS1* (Taqman primer/probe sets purchased from ABI) mRNA expression *ex vivo* via Real-Time PCR. Gene expression levels were normalized to *18S* mRNA, and relative quantification was performed using the ΔΔCt method. "Fold difference" is calculated relative to level of expression detected in the IL-1R1^{lo} subpopulation, which was arbitrarily normalized to 1. Results depicted as mean ± SEM ($n \geq 4$).

Figure S3

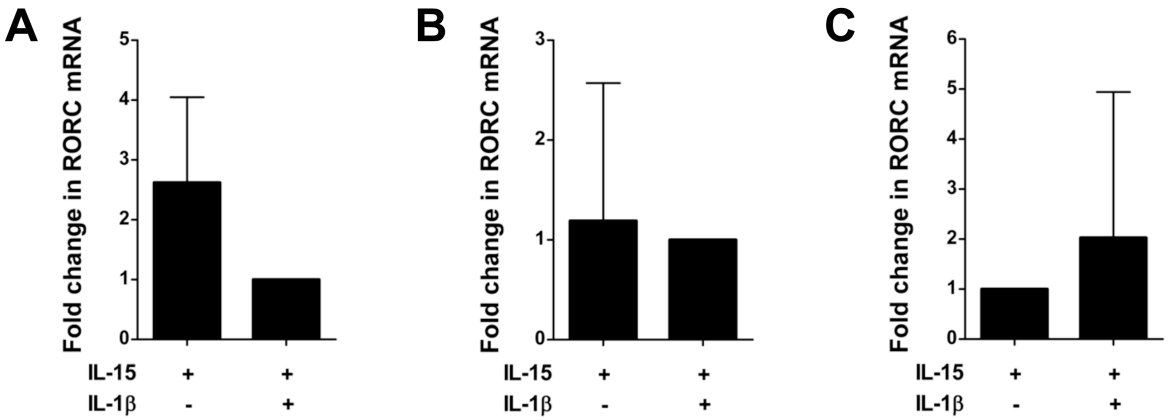

Figure S3 (related to Figure 4): *RORC* Expression Following Culture of SLT NK Developmental Intermediates in the Presence of IL-15 or IL-15 and IL-1β

Flow cytometrically sorted populations of (A) total stage 3 iNK cells, (B) IL-1R1^{hi} stage 3 iNK cells, or (C) stage 4 mature NK cells were each cultured for 14 d in the presence of IL-15 or IL-15 and IL-1β. Real-Time PCR was then used for quantitative assessment of *RORC* mRNA. Gene expression levels were normalized to *18S* mRNA, and relative quantification was performed using the ΔΔCt method. "Fold change" was calculated relative to that in the culture condition resulting in lower level of expression, which was arbitrarily normalized to 1. Results depicted as mean ± SEM ($n \geq 4$).

Figure S4

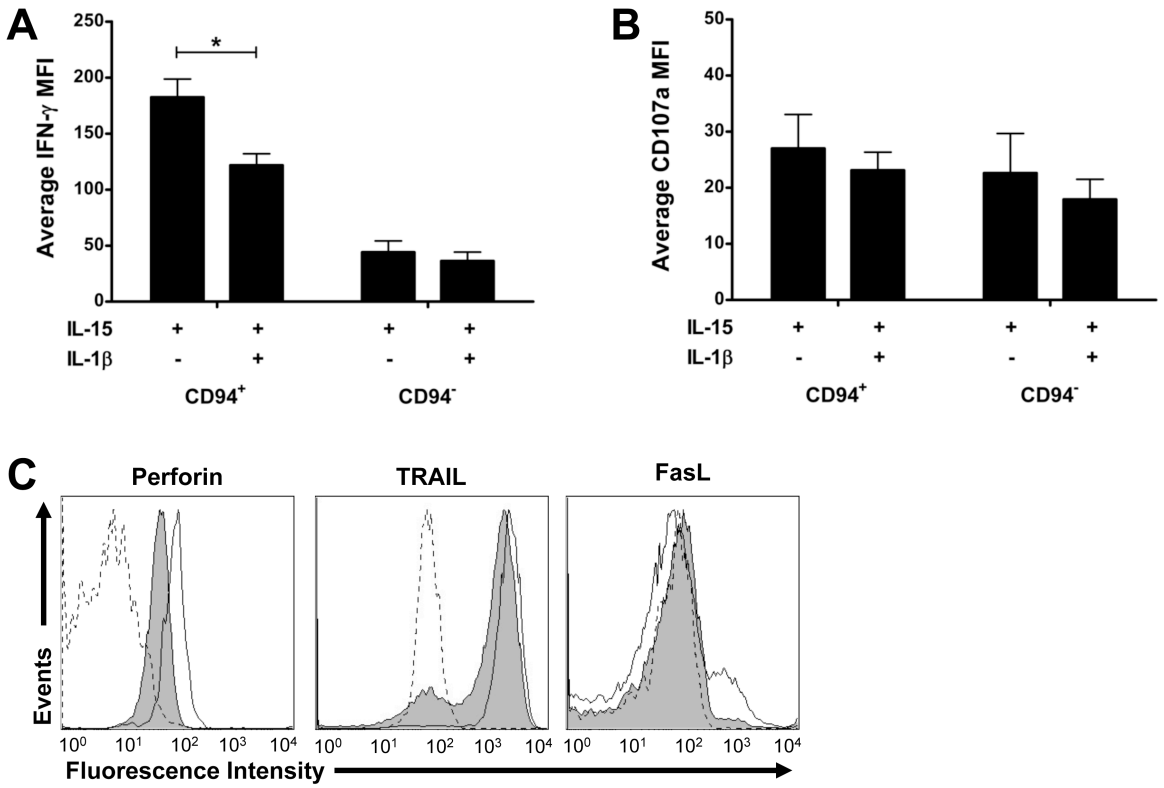

Figure S4 (related to Figure 6): IFN-γ Production and Cytotoxic Effector Function of CD94$^+$ and CD94$^-$ Populations Generated In Vitro During Culture of Total Stage 3 iNK Cells

Total stage 3 iNK cells were isolated from SLT via flow cytometry and cultured for 14 d with IL-15 or IL-15 and IL-1β.

(A and B) Cells were then stimulated as described for Figure 6 to assess acquisition of effector function. Staining was performed to measure CD94 surface expression (via flow cytometry) in combination with either (A) intracellular IFN-γ or (B) surface expression of the degranulation marker CD107a.

(A) While intensity of IFN-γ staining within the CD94$^-$ population was comparable to isotype control, IFN-γ MFI exceeded isotype within the population which had become CD94$^+$. When these cells were generated in the presence of IL-1β, IFN-γ MFI was reduced (*, $P < 0.05$). Results in A and B depicted as mean ± SEM (n ≥ 3).

(C) Alternatively, cultured cells were stained for intracellular perforin or surface expression of TNF-related apoptosis inducing ligand (TRAIL) or Fas ligand (FasL) using antibodies purchased from BD Biosciences. Histograms depict staining in a representative donor (n ≥ 4) following culture with IL-15 (empty) or IL-15 and IL-1β (shaded) compared to staining with isotype control (dashed). Staining for perforin and FasL were similar regardless of culture condition, while culture in the presence of IL-1β consistently inhibited IL-15-induced TRAIL surface expression in a minor subset of stage 3 iNK cells.

Figure S5

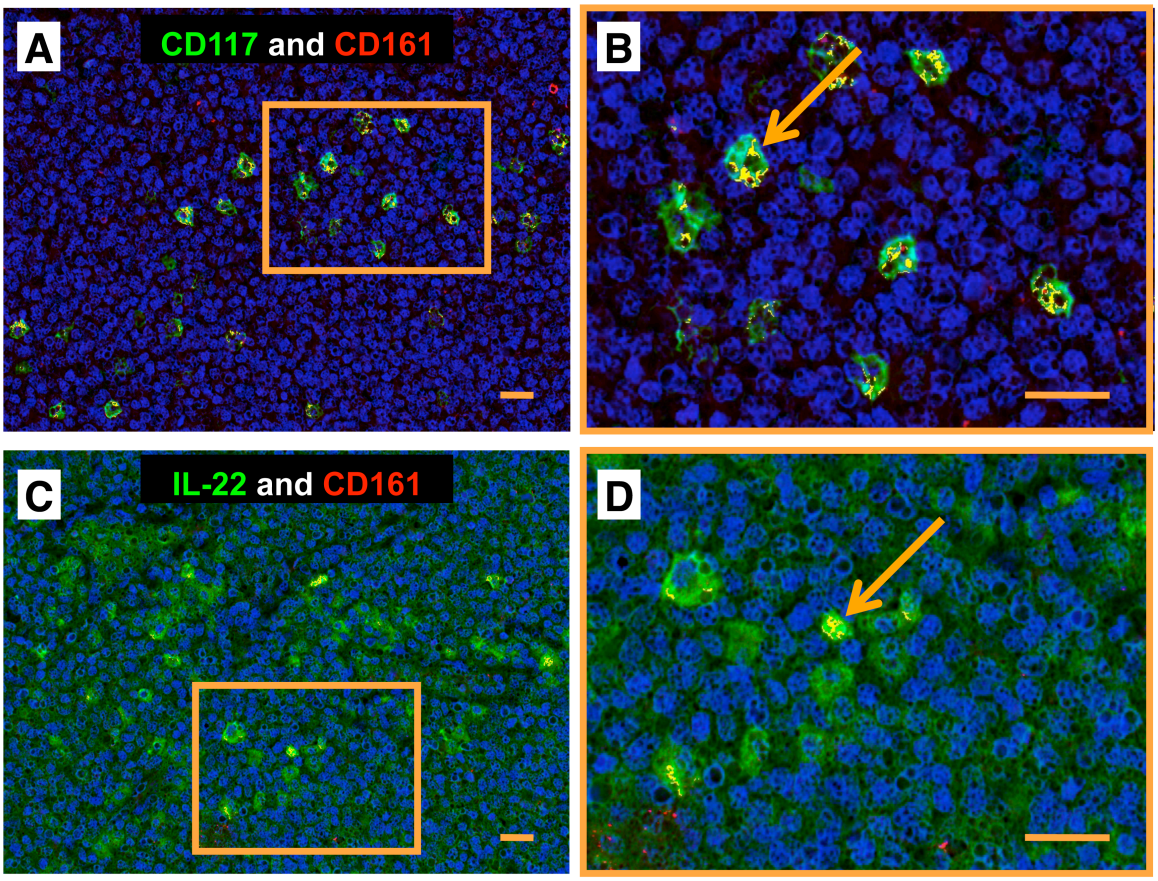

Figure S5 (related to Figure 7): Analysis of CD117$^+$ Cells within SLT
Shown in representative donor (n = 4), immunohistochemical staining was performed in serial sections of human tonsil as described for Figure 7 using the ultraView Universal system (Ventana Medical). Antigen retrieval was optimized with the Ventana cell conditioning 1 solution (Ventana Medical) for 30 minutes. The following antibodies were used in combinations indicated: α-CD117 (1:500; DakoCytomation), α-IL-22 (1:100; R&D Systems), and α-CD161 (1:333; Santa Cruz). Magnification power used for images in A and C was 400x. Higher magnifications of the insets in A and C are shown in B and D. Arrows indicate examples of co-labeled cells, which appear yellow. The CD117$^+$ cells found in SLT in the proximity of CD11c^{hi}IL-1β$^+$ cDCs (shown in Figure 7) indeed possessed a phenotype consistent with that of stage 3 iNK cells. In particular, (A,B) the majority of CD117$^+$ cells co-expressed CD161, and (C,D) IL-22 co-labeled the vast majority of CD161$^+$ cells. Bars, 30 μM.

Table S1 (related to Figure 4): Clonal Analysis of IL-1R1^{hi} and IL-1R1^{lo} Stage 3 iNK Cell Subpopulations

	IL-1R1^{hi}	IL-1R1^{lo}
Percentage of wells that grew	36.11 ± 0.55%	36.67 ± 2.54%
Percentage of wells expressing CD94*	49.35 ± 6.53%	100 ± 0%
Percentage of wells expressing IL-22**	76.77 ± 5.05%	0 ± 0%
Percentage of cells in each well expressing CD94	16.28 ± 4.34%	43.47 ± 2.95%
Percentage of cells in each well expressing IL-22	15.49 ± 1.06%	1.92 ± 0.28%

A FACSAria II was used to deposit single IL-1R1^{hi} or IL-1R1^{lo} stage 3 iNK cells directly into each well of a 96-well flat bottom plate containing GFP$^+$ murine OP9 stroma in α-MEM medium containing IL-15 and IL-1β. Half the medium was removed every 2-3 d and replaced with fresh media containing 2x cytokines. After 14 d, each of 60 replicate wells was individually assessed via flow cytometry for human CD45 and CD94 surface expression in addition to intracellular IL-22 protein. OP9 cells were excluded from analysis by gating on GFP$^-$ lymphocytes expressing human CD45. Percentage of wells that grew (a well "grew" when we detected ≥ 10 GFP$^-$CD45$^+$ events) was calculated relative to the 60 wells initially seeded with one cell. Wells were scored as positive for CD94 and/or IL-22 when the proportion of GFP$^-$CD45$^+$ lymphocytes which were CD94$^+$ or IL-22$^+$ exceeded 2% (corresponding to level of background staining detected with isotype control antibodies). Percentages of wells expressing CD94 and/or IL-22 were calculated relative to number of wells that grew. Percentages of cells in each well expressing CD94 or IL-22 represent the proportion of cells which were CD94$^+$ or IL-22$^+$ among total live cells (GFP$^-$CD45$^+$) detected in that well. As shown in Figure 4H (which depicts staining of IL-1R1^{hi} and IL-1R1^{lo} clones from a representative donor), although CD94$^+$ cells and IL-22$^+$ cells were sometimes generated in the same well, these antigens were expressed in a manner which remained mutually exclusive, and occurred on separate cells. Data summarized above represent mean ± SEM from 2 independent experiments with similar results (*, $P \leq 0.05$; **, $P \leq 0.005$; n = 3 donors).

Supplemental References

Yang, J. P., Fan, W., Rogers, C., Chatterton, J. E., Bliesath, J., Liu, G., Ke, N., Wang, C. Y., Rhoades, K., Wong-Staal, F., and Li, Q. X. (2006). A novel RNAi library based on partially randomized consensus sequences of nuclear receptors: identifying the receptors involved in amyloid beta degradation. Genomics *88*, 282-292.